biology

MDPI

Article

Comparative Analysis of Morphological, Molecular, and Physicochemical Markers to Evaluate *Trollius ledebouri* Rchb. as a Potential Alternative Source to *Trollius chinensis* Bunge for High-Quality Flos Trollii Supplements

Lianqing He [1,†], Panpan Wang [1,†], Zhen Wang [2], Lingyang Kong [1], Junbai Ma [1], Shumin Huang [1], Meitong Pan [1], Keke Yang [3], Weili Liu [1], Wei Ma [1,*] and Xiubo Liu [1,3,*]

[1] School of Pharmacy, Heilongjiang University of Chinese Medicine, Harbin 150040, China; hhelianqing@126.com (L.H.); 15134532248@163.com (P.W.); hljkly970219@163.com (L.K.); 15114516116@163.com (J.M.); hsm182375@163.com (S.H.); liuweili410@126.com (W.L.)
[2] Key Laboratory of Xinjiang Phytomedicine Resource and Utilization, Ministry of Education, School of Pharmacy, Shihezi University, Shihezi 832003, China; zhenwang@shzu.edu.cn
[3] Jiamusi College, Heilongjiang University of Chinese Medicine, Jiamusi 154007, China; yangkeke198110@163.com
* Correspondence: mawei@hljucm.edu.cn (W.M.); zyylxb@foxmail.com (X.L.)
† These authors have contributed equally to this work.

Simple Summary

Trollius chinensis Bunge is a medicinal herb whose dried flowers (Flos Trollii) exert heat-clearing and detoxifying effects. *Trollius ledebouri* Rchb., a morphologically similar species in the Great Xing'an Mountains with inconsistent regulatory status, lacks a systematic comparison with it. This study used morphological assessment, microscopy, DNA barcoding, and physicochemical analysis to explore its potential as an alternative. Results showed distinct morphological and genetic differences between the two species, but *Trollius ledebouri* Rchb. had slightly higher orientin and vitexin levels. It holds potential as a Flos Trollii alternative, requiring further metabolomic studies.

Abstract

Trollius chinensis Bunge (TCB), a perennial Ranunculaceae herb, produces Flos Trollii-dried flowers with medicinal properties including heat clearing, detoxification, and relieving oral/throat discomfort, eye pain, and cold-induced fever. TCB is mainly cultivated in northern China, while *Trollius ledebouri* Rchb. (TLR), distributed in Heilongjiang's Great Xing'an Mountains, is morphologically similar to TCB. However, their regulatory statuses are inconsistent, and comprehensive comparative studies are lacking. This study adopted morphological assessment, microscopy, DNA barcoding, and physicochemical analysis to explore whether TLR could be a potential alternative source of Flos Trollii. Key differences were identified: TLR's sepals are shorter than petals, whereas TCB's sepals and petals are nearly equal in length; TLR has brown secretory structures absent in TCB. Genetic distance analysis showed high conservation in *ITS*2 and *trnL-trnF* sequences between the two species, but *psbA-trnH* sequence divergence exceeded the 0.05 threshold. HPLC quantification revealed that TLR contained slightly higher levels of orientin and vitexin than TCB. HPLC quantification revealed that TLR contained slightly higher levels of orientin (5.370–5.377 mg/g) and vitexin (1.954–2.053 mg/g) compared to TCB (orientin: 4.493–4.620 mg/g; vitexin: 1.361–1.451 mg/g). Collectively, TLR exhibits comparable flavonoid content and holds potential as an alternative Flos Trollii source. Given the limited bioactive compounds analyzed, future research should conduct comprehensive metabolomic profiling to fully evaluate its

Check for updates

Academic Editor: Davide Tagliazucchi

Received: 12 January 2026
Revised: 5 February 2026
Accepted: 9 February 2026
Published: 14 February 2026

Copyright: © 2026 by the authors. Licensee MDPI, Basel, Switzerland. This article is an open access article distributed under the terms and conditions of the Creative Commons Attribution (CC BY) license.

phytochemical composition and medicinal value. These data establish chemotaxonomic markers for Trollius authentication in herbal medicine.

Keywords: *Trollius chinensis* Bunge; *Trollius ledebouri* Rchb.; morphological trait; pharmacognostic parameters; DNA Barcoding; physicochemical analysis

1. Introduction

Trollius chinensis Bunge (TCB) is a perennial herb of the Ranunculaceae family. Its dried flowers, referred to as Flos Trollii [1], possess significant medicinal properties [2]. Flos Trollii are documented in classical texts such as the Supplement to Compendium of Materia Medica, where they are described as bitter, cold, non-toxic, and are used to treat aphtha, sore throat, otalgia, and ophthalmalgia [3]. Currently, 16 species have been reported in China, of which 8 are endemic, predominantly found in high-altitude areas of Northeast, North, Northwest, and Southwest China [4]. TCB is primarily distributed in the northern and northeastern regions of China, including Hebei, Henan, Jilin, Liaoning, Nei Mongol, and Shanxi. *Trollius ledebouri* Rchb. (TLR) is predominantly located in Heilongjiang, Liaoning, and northeastern Inner Mongolia, as well as in Mongolia and the Russian regions of the Far East and Siberia [5]. TCB was previously included in the Pharmacopoeia of the People's Republic of China but was later removed due to resource limitations. Nevertheless, it remains recognized in several provincial standards, including the Quality Standard for Chinese Herbal Medicine in Hubei Province (2018 Edition), Tianjin Standards for the Processing of Traditional Chinese Medicine Slices (2018 Edition), and Shanghai Standards for the Processing of Traditional Chinese Medicine Slices (2018 Edition). In contrast, TLR is only accepted as a source of Flos Trollii within the Heilongjiang Province Chinese Medicinal Materials Standard (2001 Edition) and Heilongjiang Province Chinese Medicinal Materials Processing Standard (2012 Edition).

This inconsistent regulatory status, combined with overlapping geographical distributions and morphological similarities between TCB and TLR, underscores the urgent necessity for reliable authentication methods. Such methods are crucial to ensure accurate species identification and consistent quality of herbal materials. Currently, the lack of comprehensive comparative studies between TCB and TLR regarding identification and quality control further highlights a significant research gap. Traditionally, species identification relies primarily on morphological characteristics, particularly floral and fruiting attributes. Morphologically, the two species are highly similar, but can be distinguished by key floral traits: in TCB, the linear petals are typically equal to or longer than the sepals, whereas in TLR, the petals are distinctly shorter than the sepals. However, the accuracy of morphological identification is inherently limited and often depends on the experience and expertise of the taxonomic specialists involved [6]. These limitations emphasize the need for more objective and reproducible approaches.

DNA barcoding serves as a powerful identification tool, addressing the shortcomings associated with morphological methods. It is employed not only for the accurate identification of species and closely related taxa but also for the discovery of new species [6]. Compared to other identification methods, DNA barcoding exhibits high repeatability, stability, and universality, potentially facilitating the establishment of a unified database and identification platform [6]. The Internal Transcribed Spacer (*ITS*2) region is located within the nuclear ribosomal internal transcribed spacer and forms part of the non-transcribed regions of ribosomal RNA genes. This region displays considerable variability and species-specific characteristics, making it highly effective for both intraspecific and interspecific

phylogenetic analyses and species identification. The *psbA-trnH* and *trnL-trnF* sequences are chloroplast DNA regions situated between the *psbA* and *trnL* genes, respectively. These regions are frequently employed to complement identification of closely related species when the *ITS*2 region alone is insufficient [7]. Integrating nuclear and chloroplast barcodes has been successfully utilized in authenticating numerous medicinal plants, significantly improving identification accuracy. Despite the well-established DNA barcoding technology, its application within the genus Trollius remains limited.

Phytochemical studies have concurrently revealed that more than 100 compounds have been isolated from the genus *Trollius*. The primary constituents include flavonoids, organic acids, coumarins, alkaloids, and terpenoids [8]. Trollius species are traditional Chinese medicinal herbs, and their flavonoids are the main active components. Flavonoids, particularly orientin and vitexin, are the principal active compounds in Flos Trollii and exhibit significant antioxidant activity [9]. Given the morphological and ecological similarities between TCB and TLR, their phytochemical profiles may also be comparable. Nevertheless, the potential of TLR as an alternative source of Flos Trollii remains poorly studied, and a comprehensive comparison of these two species using integrated methods is currently lacking.

Thus, to address this research gap, the present study employs a multidisciplinary strategy that combines morphological observation, microscopic analysis, and DNA barcoding (using *ITS*2, *psbA-trnH*, and *trnL-trnF* regions) to authenticate and differentiate TCB and TLR. Additionally, chemical analyses were conducted using orientin and vitexin as reference standards to evaluate and compare the quality of materials derived from these two species. The primary objectives were to systematically compare the quality of TCB and TLR, assess whether TLR demonstrates comparable flavonoid content, and determine if it warrants further investigation as a potential alternative.

2. Materials and Methods

2.1. Plant Materials and Chemical Reagents

TCB and TLR, collected from different areas in Mount Wutai, Shanxi and Great Xing'an Range, Heilongjiang Province in China, were identified by Pr. Wei Ma (Heilongjiang University of Chinese Medicine, Harbin, China). Analytical grade methanol was used for sample preparation. Methanol (Analytical Grade) (Tianjin Fuyu Fine Chemicals Co., Ltd., Tianjin, China). High purity purchased from Dickma Company. Acetonitrile (chromatographic grade, Dickma Company, Beijing, China); And purified water meeting the high purity standards required for the application of high-performance liquid chromatography (HPLC) was used in the experiment, namely, Wahaha Pure Water (Hangzhou Wahaha Group Co., Ltd., Hangzhou, China). Calcium dihydrogen phosphate was provided by (Tianjin Kaimir Chemical Reagent Co., Ltd., Tianjin, China). Orison (purity $\geq$ 98%, batch number RH398763), Vitamin (purity $\geq$ 98%, batch number RH422142), and Quercetin 3-O-β-D-Galactoside (purity $\geq$ 98%, batch number RH383540) were all provided by Shanghai Yien Chemical Technology Co., Ltd. (Shanghai Yien Chemical Technology Co., Ltd., Shanghai, China). Quercetin (purity $\geq$ 98%, batch number WP24030101) was provided by (Sichuan Weikexi Biotechnology Co., Ltd., Chengdu, China).

2.2. Pharmacognostic Parameters

According to the Powder Microscopy method specified in General Rule 2001 of Part IV of the Chinese Pharmacopoeia (2020 edition), microscopic identification was performed on the floral powders of Trollius chinensis Bunge (Jinlianhua) and Trollius ledebouri Rchb. (Duanban Jinlianhua). Dried samples of each species were ground and passed through a No. 5 sieve. A small amount of the powder was placed on a glass slide, to which

2–3 drops of chloral hydrate test solution were added. After heating for clarification, a small amount of dilute glycerin was added, and a coverslip was applied. The prepared slides were observed using a YM-310 Nikon biological microscope (Nikon Instruments Co., Ltd., Shanghai, China), and images were captured for subsequent analysis. Additionally, fresh stem materials were hand-sectioned to prepare transverse sections, which were observed under the same microscope system to examine their tissue structures.

2.3. DNA Extraction, Amplification, and Sequencing

The DNA fragments corresponding to the *ITS*2, *psbA-trnH*, and *trnL-trnF* loci of the two species were extracted and subsequently amplified. Genomic DNA extracted from two *Trollius* species was amplified by polymerase chain reaction (PCR) amplification, employing universal primers and standardized conditions. Furthermore, the gene fragment data for the two plants were analyzed in conjunction with other *Trollius* species data available in the National Center for Biotechnology Information (NCBI) database [6].

Fresh leaves of TCB and TLR (100 mg each) were collected. And total DNA was extracted using a Plant Genome DNA Kit (Cat. # DP305, Tiangen Biotech (Beijing) Co., Ltd., Beijing, China) according to the manufacturer's instructions. A 25 µL PCR reaction system was prepared, containing 12.5 µL of 2× Mega Fast Taq Master Mix (Cat. # MS-P202, Msunflowers (Beijing) Co., Ltd., Beijing, China), 8.5 µL of double-distilled water (ddH2O), 1 µL of forward and reverse primers (refer to the Primer list in Table 1), and 2 µL of DNA template. Additionally, three units of Taq polymerase were utilized to amplify the marker sequences [10]. The amplification of the ITS2 region was carried out under the following thermal cycling conditions: initial denaturation at 94 °C for 4 min; 40 cycles of denaturation at 94 °C for 30 s, annealing at 58 °C for 30 s, and extension at 72 °C for 1 min; followed by a final extension at 72 °C for 5 min. In contrast, the thermal cycler conditions for the amplification of the *psbA-trnH* and *trnL-trnF* intergenic spacer regions involved 33 cycles, starting with an initial denaturation at 95 °C for 5 min, followed by denaturation at 95 °C for 20 s, annealing at 56 °C for 20 s, and extension at 72 °C for 40 s. The PCR products, along with a 2000 bp DNA marker (Shanghai Macklin Biochemical Technology Co., Ltd., Shanghai, China), were separated using 1% agarose gel electrophoresis. PCR amplification was conducted using a polymerase chain reaction analyzer Eppendorf AG 22331 Hamburg (Bole Life Medical Products (Shanghai) Co., Ltd., Shanghai, China). The amplification rates of the ITS2 sequences, psbA-trnH sequences, and trnL-trnF sequences for TCB and TLR were all 100%, demonstrating successful amplification characterized by clear and specific bands without smearing. The amplified products were subsequently sent to RiboXingke Co., Ltd. (RiboXingke Co., Ltd., Harbin, China) for sequencing.

Table 1. Primer list.

Name	5′ → 3′ Sequence	Purpose	Reference
*ITS*2-F	YGACTCTCGGCAACGGATA	Amplification of the ITS2 spacer region	[11]
*ITS*2-R	RGTTTCTTTTCCTCCGCTTA		
psbA-F	GTTATGCATGAACGTAATGCTC	Amplification of the psbA-trnH spacer region	[12]
trnH-R	CGCGCATGGTGGATTCACAATCC		
trnL-C	CGAAATCGGTAGACGCTACG	Amplification of the trnL-trnF spacer region	[13]
trnF-D	GGGGATAGAGGGACTTGAAC		

2.4. Sequence Alignment and Analysis

The original sequences were carefully proofread and assembled, and the ITS2 regions were annotated and trimmed with reference to the conserved flanking sequences (5.8 S and 28 S) utilizing CodonCode Aligner version 11.0.2 (CodonCode Co., Ltd., Centerville,

UT, USA). Multi-sequence alignments of the ITS2, psbA-trnH, and trnL-trnF regions were performed with DNAMAN 9.0 software (Lynnon BioSoft Co., Ltd., South San Francisco, CA, USA). DNA sequences of *Trollius* species were retrieved from the NCBI database for phylogenetic analysis. GC content and intra- and inter-species genetic distances based on the Kimura 2-parameter (K2P) model were calculated using MEGA v11.0 [14]. Phylogenetic trees were reconstructed with the Neighbor-Joining (NJ) method implemented in MEGA version 11.0 [15]. The phylogenetic tree was reconstructed using the Maximum Likelihood method, with branch lengths scaled according to the number of nucleotide substitutions per site. The analysis employed 1000 bootstrap replicates to assess node support, and gaps and missing data were handled using the pairwise deletion option. A site coverage cutoff of 95% was applied to include only alignment positions with sufficient data across taxa.

2.5. Physicochemical

2.5.1. Identification by Thin-Layer Chromatography

Referring to the thin-layer chromatography (TLC) identification method outlined in the General Principles of the Chinese Pharmacopoeia (2020 edition, Section 0502) [16,17]. Sample powders of TCB and TLR (0.25 g each) were accurately weighed and extracted with 25 mL of 70% ethanol under sonication (80 kHz and 400 W) for 30 min. After extraction, the solution was filtered and evaporated to dryness. The residue was then dissolved in 10 mL of water and extracted twice with n-butanol (10 mL each time). The combined extracts were evaporated to dryness in a water bath, and the residue was dissolved in 4 mL of methanol to obtain the test solution. Accurately weigh the reference substances, vitexin and orientin, and prepare the reference solution by dissolving them in methanol. Subsequently, prepare the reference herbal solution using the same methodology as that employed for the reference solution. Pipette 5 μL of the aforementioned reference herbal, test, and reference solutions onto polyamide thin films (silica gel GF254 plates measuring 100 mm × 200 mm). Utilize a developing agent composed of chloroform, acetone, glacial acetic acid, and anhydrous ethanol in a volume ratio of 4:1:3:2. After development, the plates were sprayed with a 1% $AlCl_3$ ethanol solution, heated to enhance spot visibility, and examined under ultraviolet lamp at 365 nm. The selection of a developing solvent is a critical determinant of separation efficiency in thin-layer chromatography (TLC). The retention factor (Rf) and resolution (R) represent key performance metrics for assessing the efficacy of the solvent system. The Rf value is defined as the ratio of the migration distance of a compound to that of the solvent front. Quantitative analysis of TLC plates was performed using JustTLC software 4.6, which facilitated the automatic quantification of Rf values. The analytical procedure commenced with background subtraction to improve the signal-to-noise ratio. Subsequent adjustments to image contrast and brightness were applied to enhance the visibility of chromatographic bands. Regions corresponding to separated compounds were identified, integrated, and converted into peak areas, enabling precise quantitative evaluation. This workflow supported efficient digitization and reliable quantification of chromatographic results [18].

2.5.2. Total Flavonoid Content

TCF of the extracts from TCB and TLR was determined by the aluminum nitrate colorimetric method with rutin as the standard reference. The detailed procedure was as follows: Rutin standard solutions with a mass concentration of 0.01–0.05 mg/mL were prepared to plot the standard curve. A 1.0 g portion of sample powder passed through a 60-mesh sieve was accurately weighed, mixed with 40 mL of 70% ethanol, and subjected to ultrasonic extraction at 250 W and 40 kHz for 30 min. After cooling, the extract was replenished to the original weight, filtered, and a 0.5 mL aliquot of the subsequent filtrate

was taken as the test solution. To the test solution, 1.0 mL of 5% sodium nitrite solution, 1.0 mL of 10% aluminum nitrate solution, and 10 mL of 4% sodium hydroxide solution were added sequentially, with an interval of 6 min between each addition. After the addition, the mixture was diluted to 25 mL with 70% ethanol and allowed to stand for 15 min. Using a reagent blank as the reference, the absorbance was measured at a wavelength of 510 nm with a UV-Vis spectrophotometer (Shanghai Jingke Industrial Co., Ltd., Shanghai, China). TCF was calculated according to the rutin standard curve with the regression equation Y = 10.306X + 0.0083 (R^2 = 0.9992), and the results were expressed as milligrams of rutin equivalents per gram of dry sample (mg/g).

2.5.3. HPLC Instrumentation and Chromatographic Conditions

An appropriate amount of orientin and vitexin was accurately weighed and dissolved in 70% methanol to prepare standard solutions with concentrations of 120 μg/mL and 100 μg/mL, respectively. Each solution was filtered using a 0.45 μm membrane filter. Approximately 0.3 g of the powdered sample (passed through a 60-mesh sieve) was placed in a conical flask containing 50 mL of an 80% (*v*/*v*) ethanol solution. The flask was weighed and subjected to ultrasonic treatment for 60 min at 250 W and 40 kHz. After cooling to room temperature, the weight was replenished with the same solvent, and the mixture was filtered. The resulting filtrate was accurately measured to a volume of 25 mL and evaporated using a water bath. The residue was dissolved in 25 mL of water and extracted twice with 30 mL of ethyl acetate. The extracts were combined, evaporated, and the resulting residue was dissolved in 50 mL of methanol before being filtered again using a 0.45 μm syringe filter.

HPLC analysis was carried out on a Thermo U-3000 HPLC system (Thermo Fisher Scientific Co., Ltd., Shanghai, China). An Agilent TC-C18 column (150 × 4.6 mm, 5 μm) was maintained at a temperature of 40 °C. The mobile phase consisted of acetonitrile (A) and 0.2% glacial acetic acid (B) in a volume ratio of 13:87 (*v*/*v*) and was delivered at a flow rate of 1.0 mL/min. The injection volume was 5 μL, and detection was established at 349 nm. The total run time is 30 min.

2.5.4. HPLC Method Validation

The HPLC method that was developed underwent validation in accordance with the guidelines established by the International Council for Harmonisation (ICH) pertaining to the validation of analytical methods. The validation parameters assessed included linearity, accuracy, precision, specificity, limit of detection (LOD), and limit of quantification (LOQ).

Accurately pipette a specified volume of the Orientin standard solution to prepare a standard solution with a concentration of 60 μg/mL. Subsequently, dilute this solution to achieve six distinct concentrations: 2 μg/mL, 12 μg/mL, 36 μg/mL, 60 μg/mL, 80 μg/mL, and 108 μg/mL. Similarly, accurately pipette a designated volume of the Vitexin standard solution to prepare a standard solution with a concentration of 50 μg/mL, and then dilute it to obtain six concentrations: 1 μg/mL, 10 μg/mL, 30 μg/mL, 50 μg/mL, 70 μg/mL, and 90 μg/mL. Following their preparation, the solutions were filtered through a 0.45 μm membrane and analyzed by HPLC under the specified chromatographic conditions. The peak area integration values should be plotted as the dependent variable (Y) against the injection volumes, which serve as the independent variable (X). Subsequently, linear regression equations for each component must be calculated. A fixed concentration of a mixed standard solution should be injected six times consecutively to evaluate the precision of the method. Additionally, six replicates of any sample should be prepared and injected to assess the repeatability of the method. Stability studies on the same test solution should be conducted by injecting it at intervals of 0, 4, 8, 12, 24, and 36 h. The accuracy of the

method will be evaluated by analyzing three spiked samples with known concentrations of the targeted phytochemicals and calculating the percent recovery. LOD and LOQ will be determined based on the standard deviation of the response and the slope of the calibration curve, with the formulas LOD = 3.3 δ/S and LOQ = 10 δ/S. In this context, δ represents the standard deviation of the response value, which can be substituted with the standard deviation of the intercept of the calibration curve.

3. Results

3.1. Pharmacognostic Parameters

The data corresponding to the pharmacognostic parameters are summarized in Figures 1–3.



Figure 1. (**A**) is TLR, (**B**) is TCB. The following descriptions pertain to various morphological aspects of the plants: (I) Morphology of the entire plant; (II) Basal leaves; (III) Cauline leaves; (IV) Locular capsule; (V) Stamen; (VI) Perianth flank; (VII) The petals are in contrast to the sepals, which are narrowly strip-shaped, while the sepals themselves exhibit an obovate form; (VIII) Anatomy of a complete flower; (IX) Lateral side of the flower; (X) Ventral side of the flower; (XI) The flower has been longitudinally sectioned to illustrate the positioning of each floret on the receptacle.

3.1.1. Morphological Identification

The two collected *Trollius* species are biennial herbaceous plants with highly similar morphological characteristics. Based on the morphological descriptions provided in the Flora of China (FOC), we collected specimens during the blooming period of TCB and TLR in June, and accurately identified each species based on their flowers and leaves (Figure 1).

A diagnostic key was developed to aid in the morphological identification of TCB and TLR, as outlined below (Table 2):

1. Glabrous throughout.

1

2. Basal leave long-petioles; leaf blade pentagonal, cordate at base, deeply tripinnatisect; segments extending nearly or slightly beyond the midvein, distinc; median segment rhombic, apex acute. Cauline leaves similar to basal leaves; upper leaves gradually reduced.

2

3. Flowers solitary or in 2–3-flowered sparse cymes, dried specimens non-green; sepals elliptic-ovate to ovate, apex rounded.

3

4. Basal leaves margins serrate; leaves typically tripinnate with unequally triangular-acute teeth; lateral lobes flabellate, deeply divided twice near base; upper deep lobe resembling median lobe, lower deep lobe oblique rhombic.

Trollius chinensis Bunge

Basal leaves with marginal lobes small, toothed triangular; lateral lobes obliquely flabellate, unequally deeply divided near base.

Trollius ledebouri Rchb.

4

5. The stem leaves have long petioles, with short petioles or no petioles.

Trollius chinensis Bunge

The stem leaves sessile.

Trollius ledebouri Rchb.

5

6. The flowers are golden yellow, with their petals ranging in number from 18 to 21 and displaying striped patterns. The calyxes possess triangular or indistinct teeth, with their quantity typically ranging from 10 to 15, although a minimum of 6 and a maximum of 19 calyxes may be observed. The petals are either slightly longer than or nearly equal in length to the calyxes, and they may occasionally be shorter than the sepals, exhibiting a linear morphology. The stamens measure between 5 and 11 mm in length, while the number of carpels ranges from 20 to 30. The capsule fruit is approximately 1 to 1.2 cm in length with a beak measuring about 1 mm.

Trollius chinensis Bunge

The flowers are yellow, with their petals ranging in number from 10 to 22. The petals are linear in shape and taper at the apex. The calyx does not possess triangular or indistinct teeth, and the number of calyx lobes ranges from 5 to 10. The petals are longer than the stamens but shorter than the calyx lobes, maintaining a linear form that narrows at the apex. In TLR, the stamens measure approximately 9 mm in length, while the number of carpels varies from 20 to 28. The capsule fruit is approximately 7 mm in length, with a beak measuring about 1 mm.

Trollius ledebouri Rchb.

6

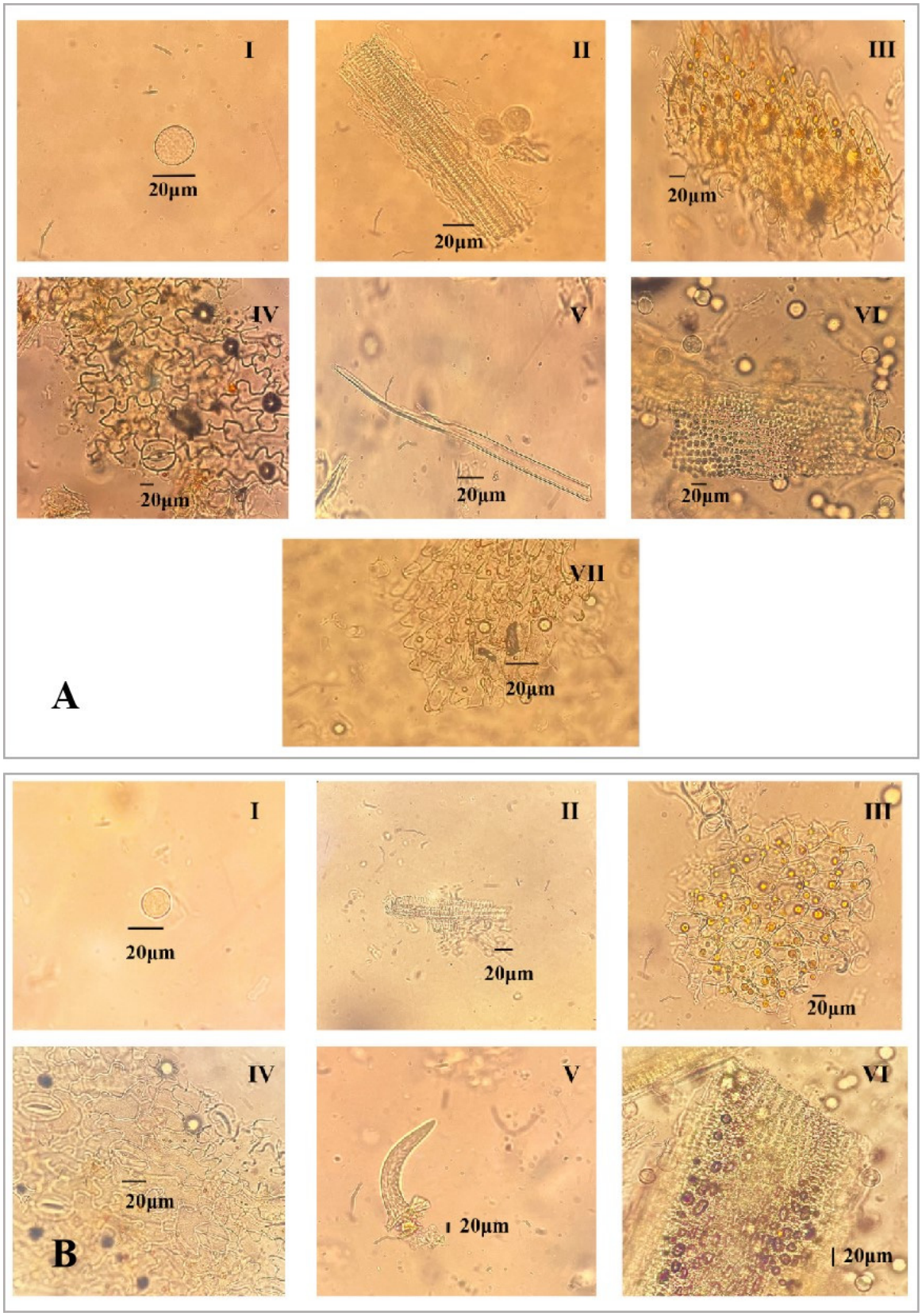


Figure 2. The microscopic characteristics in detail: (**A**) TLR, (**B**) TCB. Note: (**I**) Pollen grains; (**II**) Spiral vessels; (**III**) Calyx epidermal cells—apical fragments; (**IV**) Subsidiary cell; (**V**) trichomes; (**VI**) Epidermal cells; (**VII**) Brown block.

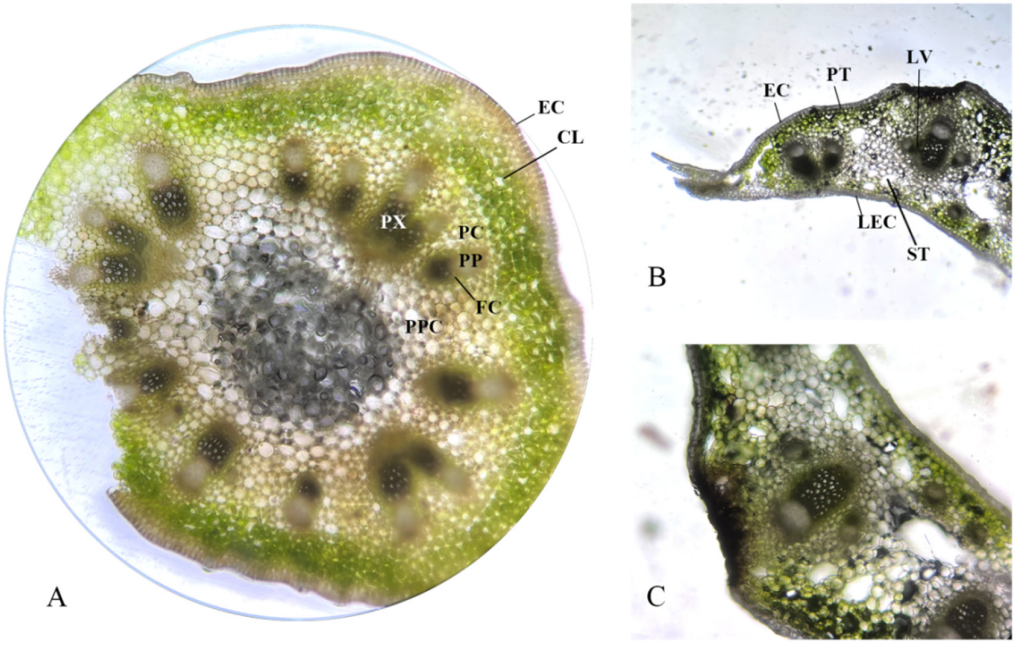


Figure 3. Representative cross-sectional views of stem and leaf tissues of TCB and TLR. (**A**) Stem cross-section of TCB showing epidermis (EC), cortex (CL), vascular bundles with primary phloem (PP) and primary xylem (PX), and pith parenchyma (PPC). (**B**) Leaf cross-section of TCB illustrating upper and lower epidermis (EC, LEC), palisade tissue (PT), spongy tissue (ST), and a vascular bundle (LV). (**C**) Leaf cross-section of TLR.

Table 2. Key morphological diagnostic characteristics distinguishing TCB and TLR.

Morphological Characters	TCB	TLR
Whole Plant Hairiness	Glabrous throughout	Glabrous throughout
Basal Leaf Characteristics	Long-petioled; pentagonal, cordate-based, deeply tripinnatisect; median segment rhombic-acute; lateral lobes obliquely flabellate, unequally lobed at base	Long-petioled; pentagonal, cordate-based, deeply tripinnatisect; serrate, tripinnate; lateral lobes flabellate, twice-divided at base
Cauline Leaf Characteristics	Similar to basal leaves, upper ones reduced; long-petioled, upper short-petioled or sessile	Similar to basal leaves, upper ones reduced; sessile
Inflorescence and Dried Specimen Color	Solitary or 2–3-flowered sparse cymes; dried specimens non-green	Solitary or 2–3-flowered sparse cymes; dried specimens non-green
Sepal Characteristics	10–15 (rarely 6–19); elliptic-ovate, rounded apex; with triangular/indistinct teeth	5–10; elliptic-ovate, rounded apex; without triangular/indistinct teeth
Petal Characteristics	18–21, linear, striped; equal/slightly longer than sepals (occasionally shorter)	10–22, linear, apex-tapering; longer than stamens, shorter than sepals
Stamen Length	5–11 mm	5–9 mm
Carpel Number	20–30	20–28
Fruit Characteristics	Follicle, 10–12 mm; beak 1 mm	Follicle, 7 mm; beak 1 mm

3.1.2. Microscopy Analyze

The microscopic examination revealed that the powders of TCB and TLR shared highly comparable anatomical features, consistent with a previous study [19]. However, a

discernible difference was noted in their macroscopic powder coloration: TCB presented a golden yellow hue, whereas TLR appeared marginally darker with an orange-yellow tint. Detailed observation under the microscope showed that both powders contained: Spiral vessels, predominantly occurring in bundles with occasional solitary vessels; Pollen grains that were abundant, subglobose to trigonal in shape with a slightly convex surface, and most grains were light yellow or colorless, and a portion exhibited three distinct germination pores [20]. Vessels occurred mostly in bundles, with fewer solitary ones, and were primarily of the spiral type. Calyx epidermal cells (apical fragments) exhibited a light yellow coloration and distinct papillary protrusions. The calyx epidermal cells exhibited an undulate morphology containing golden-yellow inclusions, with anomocytic stomata that were subrounded to circular in shape, characterized by curved anticlinal walls and surrounded by 4–5 subsidiary cells. Additionally, some cell cavities contain nearly round, golden yellow inclusions and brown blocks [19,21]. Unicellular trichomes were rod-shaped; the upper epidermal cells of the petals were rectangular with longitudinal parallel striations and golden-yellow inclusions; no stomata were observed; however, no brown blocks were detected in TCB [22] (see Figure 2).

No significant anatomical differences were observed in the leaf and stem cross-sections between TCB and TLR. The leaves are bifacial: the adaxial side differentiates into palisade tissue, while the abaxial side forms spongy tissue. Leaf cross-sections show an absence of collenchyma, the presence of protrusions, and multiple vascular bundles. Both the upper and lower epidermises' leaf cross-sections show layers of tightly arranged rectangular to irregular cells, with a higher density of stomata found on the lower epidermis. Beneath the upper epidermis lies a well-organized layer of cylindrical palisade cells. The spongy mesophyll occupies most of the area below the palisade layer; it is composed of irregularly shaped, thin-walled oval or round cells with large intercellular spaces and numerous cavities [23–25] (see Figure 3). The stem contains multiple collateral vascular bundles of varying sizes, separated by broad and narrow rays. Phloem cells are small and densely arranged, whereas xylem vessels are aligned linearly and interspersed with abundant wood fibers. The pith parenchyma is hollow [24] (see Figure 3, Table 3).

3.2. DNA Barcoding-Based Identification and Authentication

Despite morphological similarities, phytochemical divergence between TCB (n = 3) and TLR (n = 3) remains untested, addressed here via integrated markers.

3.2.1. ITS2 Sequence Characteristics

Among these samples, no mutated site could be discovered in TCB and TLR. The sequence similarity of plants in the genus *Trollius* is 99.56%. The full-length range of ITS2 in genus *Trollius* is 206 bp–219 bp, with an average length of 207 bp. GC content of 54.59–55.29%, resulting in an average GC content of 55.07%. The intraspecific inheritance of genus *Trollius* is relatively stable. In addition, the NJ tree was constructed to discriminate medicinally important species using all 41 ITS2 sequences, which included six sequences from experimental samples and other *Trollius* sequences obtained from NCBI. Four species (*Caltha natans*, *Caltha palustris*, *Calathodes oxycarpa*, *Calathodes palmata*) from the Ranunculaceae family were used as the outgroup (see Figure 4).

3.2.2. psbA-trnH Sequence Characteristics

Among the analyzed samples, a total of 22 mutated sites were identified in the TLR sequences. The similarity of the trnL-trnF sequences among plant species in the genus *Trollius* is 83.13%. The length of the psbA-trnH region within the genus *Trollius* ranges from 167 bp to 342 bp, with an average length of 304 bp. The GC content varies between 28.65% and 34.73%, resulting in an average GC content of 31.43%. The NJ tree was constructed

to discriminate medicinally important species using all 25 psbA-trnH sequences, which included six sequences from experimental samples and other *Trollius* sequences obtained from NCBI. One species (*Caltha palustris*) from the Ranunculaceae family was used as the outgroup (see Figure 5).

Table 3. Comparative microscopic characteristics of the floral powder of TCB and TLR.

Feature Categories and Specific Features	TCB	TLR
I. Macroscopic Powder Characteristics Powder Color	Golden yellow	Orange-yellow, slightly deeper in hue
II. Microscopic Characteristics of Floral Powder Spiral Vessels	Predominantly aggregated in bundles, occasionally solitary	Predominantly aggregated in bundles, with fewer solitary individuals
Pollen Grains	Abundant, subglobose to trigonal in shape, with a slightly convex surface; mostly light yellow or colorless, and some bearing 3 distinct germination pores	Consistent with those of TCB
Calyx Epidermal Cells	Light yellow, with distinct papillary protrusions, undulate cell contours, and containing golden-yellow inclusions	Consistent with those of TCB
Stomata Type	Anomocytic, subrounded to circular, with curved anticlinal walls and surrounded by 4–5 subsidiary cells	Consistent with those of TCB
Non-glandular Trichomes	Unicellular and rod-shaped	Unicellular and rod-shaped
Cell Cavity Inclusions	Containing nearly round golden-yellow inclusions; brown blocks absent	Containing nearly round golden-yellow inclusions and brown blocks
Petal Upper Epidermal Cells	Rectangular, with longitudinal parallel striations and golden-yellow inclusions; stomata absent	Consistent with those of TCB
III. Leaf Cross-Sectional Characteristics Leaf Type	Bifacial (dorsiventral) leaf; adaxial surface differentiated into palisade tissue, and abaxial surface developed into spongy tissue	Consistent with that of TCB
Overall Structure	Collenchyma absent, with protrusions, and containing multiple vascular bundles	Consistent with that of TCB
Epidermal Cells and Stomata	Both upper and lower epidermises consist of a single layer of tightly arranged rectangular to irregular cells; stomatal density is higher on the lower epidermis	Consistent with that of TCB
Mesophyll Tissue	A well-organized layer of cylindrical palisade cells lies beneath the upper epidermis; the spongy mesophyll occupies most of the area below the palisade layer, composed of irregular, thin-walled oval or round cells with large intercellular spaces and numerous cavities	Consistent with that of TCB
IV. Stem Cross-Sectional Characteristics Vascular Bundles	Containing multiple collateral vascular bundles of varying sizes, separated by broad and narrow rays	Consistent with those of TCB
Phloem and Xylem	Phloem cells are small and densely arranged; xylem vessels are linearly aligned, interspersed with abundant wood fibers	Consistent with those of TCB
Pith Parenchyma	Hollow	Consistent with that of TCB

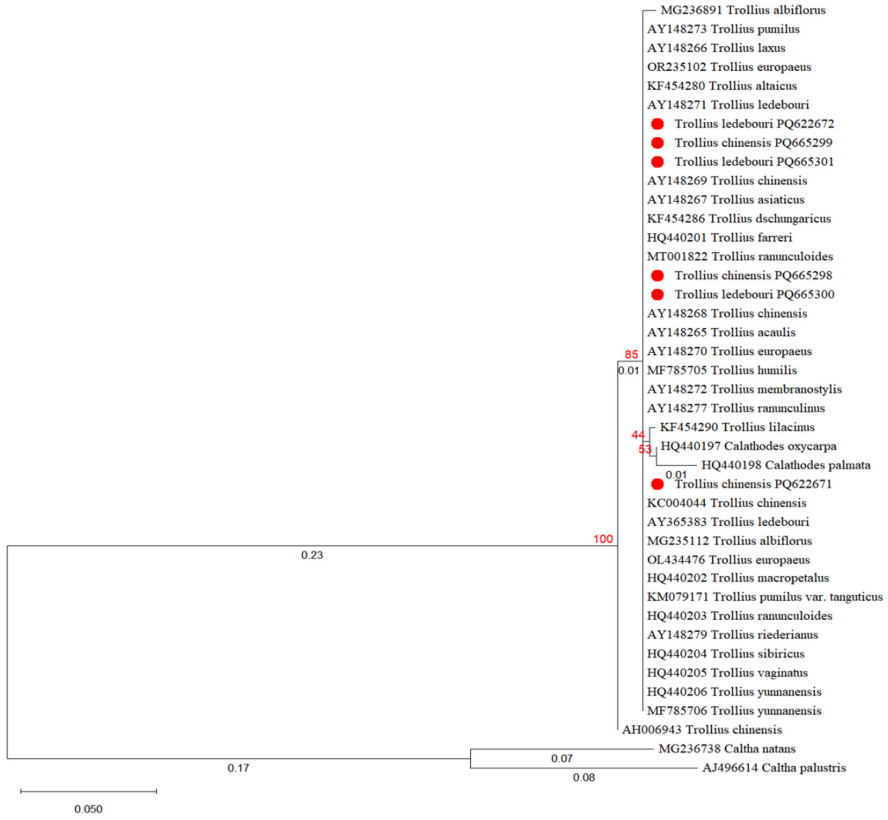


Figure 4. Phylogenetic tree of *Trollius* species inferred from ITS2 sequences. The tree is drawn to scale, with branch lengths measured in the number of substitutions per site (see scale bar). Nodes with bootstrap support greater than 50% are labeled. Branch lengths in the phylogenetic tree represent the number of nucleotide substitutions per site, with longer branches indicating greater evolutionary divergence. Sequences generated in this study are highlighted with red dots.

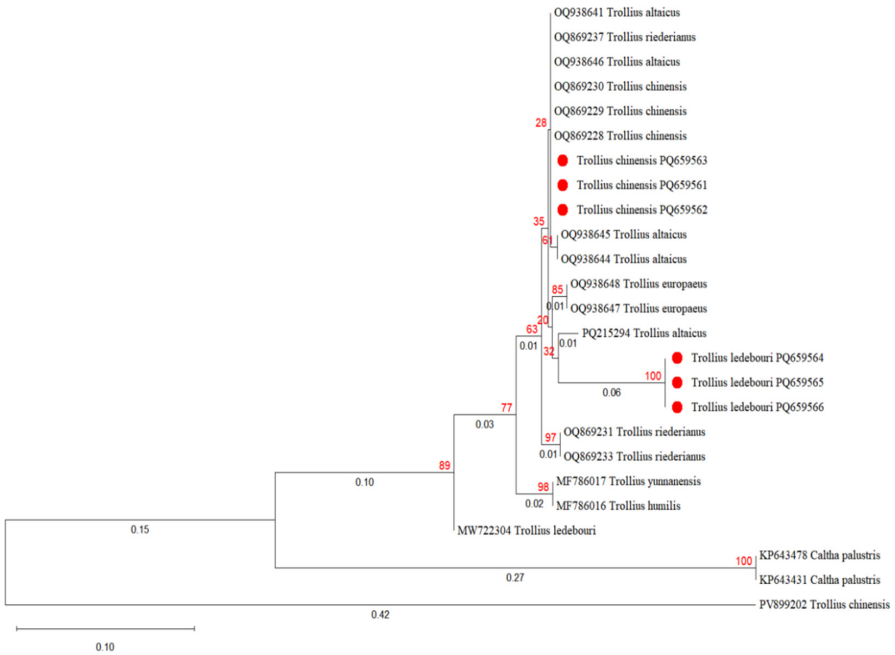


Figure 5. Phylogenetic tree of *Trollius* species inferred from psbA-trnH sequences. The tree is drawn to scale, with branch lengths measured in the number of substitutions per site (see scale bar). Nodes with bootstrap support greater than 50% are labeled. Branch lengths in the phylogenetic tree represent the number of nucleotide substitutions per site, with longer branches indicating greater evolutionary divergence. Sequences generated in this study are highlighted with red dots.

3.2.3. *trnL-trnF* Sequence Characteristics

Among the analyzed samples, one mutated site was identified in TLR. The similarity of the *trnL-trnF* sequences among plants of the genus *Trollius* is 94.60%, indicating a relatively stable pattern of intraspecific inheritance. The total length of the *trnL-trnF* sequence in plants of the genus *Trollius* ranges from 414 bp to 448 bp, with an average length of 427 bp. The GC content varies between 33.41% and 34.62%, yielding an average content of 34.29%. The NJ tree was constructed to discriminate medicinally important species using all 39 *trnL-trnF* sequences, which included six sequences from experimental samples and other *Trollius* sequences obtained from NCBI. Tour species (*Caltha natans*, *Caltha palustris* var. membranacea, *Calathodes oxycarpa*, *Calathodes palmata*) from the Ranunculaceae family were used as the outgroup (see Figure 6).

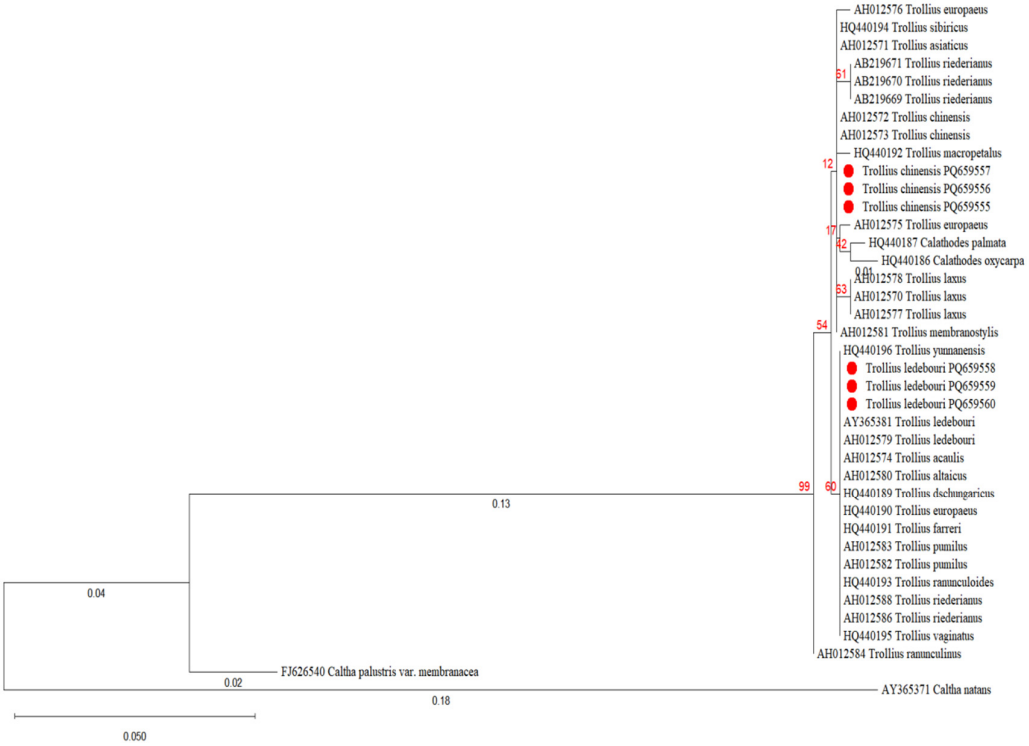


Figure 6. Phylogenetic tree of *Trollius* species inferred from *trnL-trnF* sequences. The tree is drawn to scale, with branch lengths measured in the number of substitutions per site (see scale bar). Nodes with bootstrap support greater than 50% are labeled. Branch lengths in the phylogenetic tree represent the number of nucleotide substitutions per site, with longer branches indicating greater evolutionary divergence. Sequences generated in this study are highlighted with red dots.

3.2.4. Intra-Specific and Inter-Specific Genetic Divergence Analyses

We calculated genetic distances based on the Kimura 2-parameter (K2P) model for a dataset that included newly sequenced samples of TCB and TLR and complemented by related Trollius sequences from NCBI. For the *ITS*2 region, the intraspecific genetic distances were 0.000 for TLR and 0.003 for TCB, with an overall intraspecific range of 0 to 0.005. The average interspecific distance was 0.0008 (range: 0–0.0074). In the *psbA-trnH* region, intraspecific distances reached 0.0094 for TLR and 0.2109 for TCB, with values ranging from 0 to 0.2109 across all intraspecific comparisons. The average interspecific distance was 0.0689 (range: 0–0.1576). Within the trnL-trnF region, both TCB and TLR exhibited intraspecific distances of 0.000, and the overall intraspecific variation spanned from 0 to 0.0040. The average interspecific distance was 0.0022 (range: 0–0.0055).

To evaluate the discriminatory power of the three candidate DNA barcodes, the study employed violin plots to compare the distributions of intraspecific and interspecific genetic variation within the genus *Trollius* (Figure 7). The analysis revealed distinct patterns of distribution separation between intra- and interspecific genetic variations. The ITS2 region showed a clear barcode gap, with intra-specific distances tightly clustered near zero and inter-specific distances distributed across higher values, indicating minimal overlap. The *psbA-trnH* spacer exhibited the most distinct separation, with a broad intra-specific variation and a shifted inter-specific distribution toward higher values, forming a well-defined barcode gap with no overlap. In contrast, the *trnL-trnF* region displayed extensive overlap between intra- and inter-specific distributions, with both concentrated at low values, suggesting the absence of a barcode gap (Table 4).

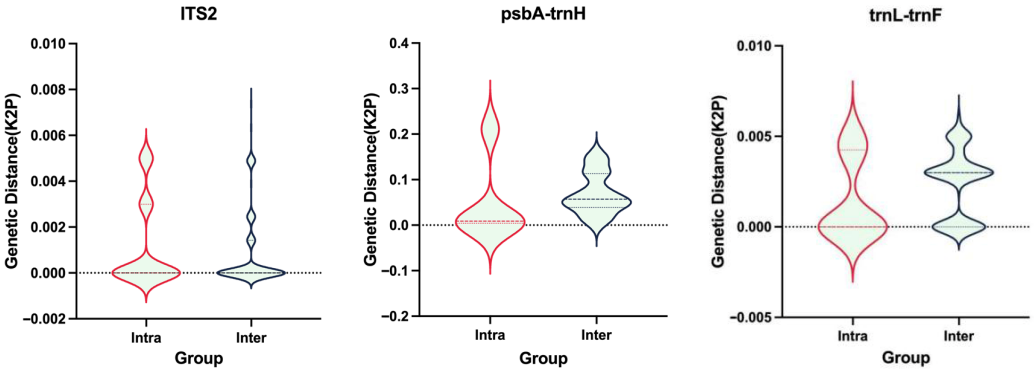


Figure 7. Violin plots depicting the distribution of intra-specific (blue) and inter-specific (red) genetic distances for the ITS2, psbA-trnH, and trnL-trnF regions. Note: (I) The width of each violin represents the density of the data. (II) The red/blue dots indicate the median genetic distance.

Table 4. Genetic Distances of Intra- and Inter-specific Variations in Three DNA Barcodes of *Trollius*.

Sequences	Intraspecific Distances				Interspecific Distance			
	Average	Range	TLR	TCB	Average	Range	TLR vs. TCB	TCB vs. TLR
ITS2	0.0003	0–0.0050	0.0000	0.0028	0.0008	0–0.0074	0.0014	0.0010
psbA-trnH	0.0574	0–0.2109	0.0094	0.2109	0.0689	0–0.1576	0.1576	0.0244
trnL-trnF	0.0015	0–0.0050	0.0000	0.0000	0.0022	0–0.0055	0.0025	0.0027

Note: (I) The intra- and inter-specific distances shown in this table were computed using the Kimura 2-parameter (K2P) model in MEGA software. (II) The two distinct values for the same species pair (e.g., TCB vs. TLR and TLR vs. TCB) result from the use of the Pairwise deletion option for gap/missing data treatment during distance calculation.

3.3. TLC Analysis

TLC analysis revealed no notable differences in the chemical profiles among the tested varieties of Trollius, including TCB and TLR. Under ultraviolet light at 365 nm, both the test samples of TLR and TCB, along with the Flos Trollii reference standard and the standard compounds (orientin and vitexin), exhibited green fluorescent spots at corresponding positions, indicating consistent chromatographic behavior and chemical composition (Figure 8).

The TLC method successfully achieved effective separation of orientin and vitexin. Under the optimized conditions, both compounds displayed clear and well-resolved spots. The measured retardation factor (Rf) values ranged from 0.168 to 0.363 for orientin and from 0.549 to 0.642 for vitexin (Figure 9). The lower Rf value of orientin suggests higher polarity, while the higher Rf value of vitexin indicates comparatively lower polarity, a finding consistent with the structural difference in the number of hydroxyl groups in

their aglycone moieties. The analysis was performed in triplicate (S1-T2) to ensure the reproducibility and reliability of the results.

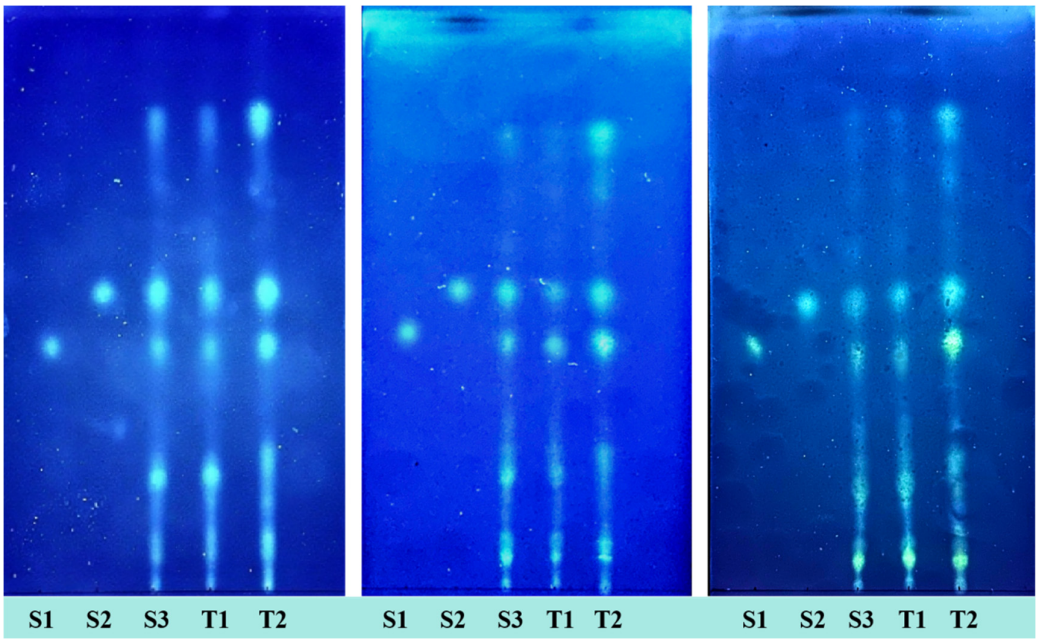


Figure 8. Thin-layer identification map of TCB and TLR under 365 nm UV light. (S1. Orientin, S2. Vitexin, S3. Reference of Flos Trollii, T1. TCB, T2. TLR).

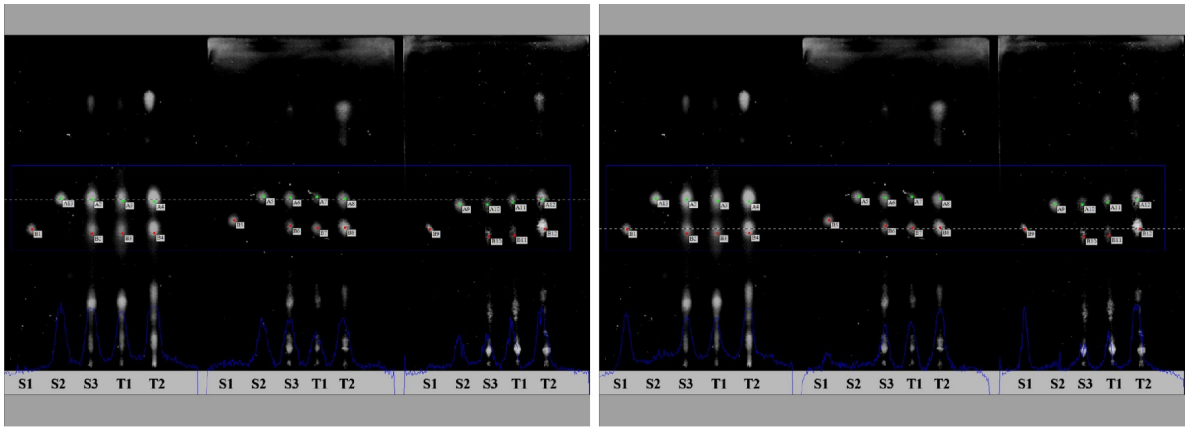


Figure 9. Thin-layer identification map of TCB and TLR, with Rf values detected using JustTLC. The green spots represent the vitexin reference, and the red spots represent the orientin reference. (S1. Orientin, S2. Vitexin, S3. Reference of Flos Trollii, T1. TCB, T2. TLR.).

3.4. Physicochemical Analysis

3.4.1. Total Flavonoid Content

TCF of TCB is 1.176–1.202 mg/g, and TCF of TLR is 1.195–1.212 mg/g. A significant linear correlation was observed between the mass concentration of TFC and the peak area. Specific TCF data are shown in Table 5.

3.4.2. HPLC Experimental Design and Treatments

The HPLC analytical results indicated that orientin exhibited a mean retention time of 14.812 ± 0.052 min (n = 3). A strong linear relationship was observed between the mass concentration of orientin and the corresponding peak area over the range of 1–54 μg/mL, with a regression equation of Y = 0.2145x + 0.0885 (R^2 value of 0.9994). Similarly, vitexin displayed a mean time of 22.042 ± 0.070 min (n = 3). A linear relationship between the

concentration of vitexin (1–45 µg/mL) and the corresponding peak area was established, following the regression equation Y = 0.1908x + 0.0395, with an R^2 value of 0.9991. A detailed summary of the method validation parameters is presented in Table 6. The limits of detection (LOD) and quantification (LOQ) for orientin were ascertained to be 1.36 µg/mL and 4.12 µg/mL, respectively, and for vitexin, these values were determined to be 0.683 µg/mL and 2.07 µg/mL, respectively. The LOD and LOQ were calculated based on the standard deviation of the intercept of the calibration curve (δ) and the slope of the calibration curve (S). The LOD and LOQ were calculated using the following formulas: LOD = 3.3 δ/S and LOQ = 10 δ/S, where δ represents the standard deviation of the intercept of the calibration curve, and S denotes the slope of the calibration curve. The recovery rates, which reflect the accuracy of the method, spanned from 98% to 100%. Method precision, expressed as the relative standard deviation (RSD), was found to be less than 1%. Comparative analysis of the medicinal fractions revealed that the concentrations of orientin and vitexin in the TLR were slightly elevated in comparison to TCB fractions ($p < 0.05$). As detailed in Table 7, the HPLC analysis demonstrated that the content of orientin in TCB varied between 1.498% and 1.540%, and in TLR, it ranged from 1.792% to 1.817%. Correspondingly, the vitexin content in TCB was found to range from 0.454% to 0.484%, and in TLR, it varied between 0.651% and 0.684%. As shown in Figure 10, the peak area corresponding to orientin and vitexin in both TCB and TLR samples is presented alongside the standard curve. The method validation results confirm that the employed HPLC method is reliable and meets all predefined validation criteria. The HPLC method exhibits exceptional linearity, accuracy, and repeatability. Furthermore, the stability of the two chemical components was preserved over a duration of 36 h, highlighting the robustness of the method. As a result, this HPLC method is deemed appropriate for the precise quantitative analysis of the two components.

Table 5. TFC values of TCB and TLR extracts.

Specie	Absorbance	TFC (mg/g)	Average (mg/g)
TLR1	0.501	1.195	
TLR2	0.502	1.198	1.202 ± 0.002
TLR3	0.508	1.212	
TCB1	0.493	1.176	
TCB2	0.504	1.202	1.189 ± 0.002
TCB3	0.499	1.190	

Note: The values are expressed as mean ± SD (n = 3) milligrams of rutin equivalents per gram of dry plant material (mg/g).

Table 6. A quantitative analysis of TCB and TLR extracts using HPLC: Validation Data.

Linearity and Sensitivity					
Compound	**Linearity Equation**	**Determination Coefficient (R^2)**	**Linearity Range (µg/mL)**	**LOD (µg/mL)**	**LOQ (µg/mL)**
Orientin	Y = 0.2145x + 0.0885	0.9994	2–108	1.360	4.12
Vitexin	Y = 0.1908x + 0.0395	0.9991	1–90	0.683	2.07
Precision	Amount (µg/mL)	Peak Area	Time	Peak Area	
Compound		RSD 0.967%		RSD 0.683%	
Orientin	24	5.0028	0 h	5.0801	
		5.1171	4 h	5.0606	
		5.0961	8 h	5.0713	
		5.1488	12 h	5.1170	
		5.0730	24 h	5.0418	
		5.0910	36 h	5.0154	

Table 6. *Cont.*

Linearity and Sensitivity					
Compound	**Linearity Equation**	**Determination Coefficient (R^2)**	**Linearity Range (µg/mL)**	**LOD (µg/mL)**	**LOQ (µg/mL)**
	Amount (µg/mL)	Peak Area RSD 0.979%	Time	Peak Area RSD 0.973%	
Vitexin	10	1.9814	0 h	1.8936	
		1.9481	4 h	1.9603	
		1.9311	8 h	1.9433	
		1.9783	12 h	1.9905	
		1.9553	24 h	1.9675	
		1.9671	36 h	1.9793	
Compound	% Recovery Spike level-1		level-2		level-3
Orientin	99.83		99.65		99.72
Vitexin	99.23		99.48		98.59

Table 7. HPLC-based quantitative analysis of TCB and TLR extracts.

HPLC Analysis							
Phytochemical	**RT (Min)**	**Amount Present in Methanolic Extract (% and mg/g)**					
		TCB1	TCB2	TCB3	TLR1	TLR2	TLR3
Orientin	14.812 ± 0.052	1.540%	1.531%	1.498%	1.792%	1.817%	1.812%
		4.620	4.594	4.493	5.377	5.371	5.370
vitexin	22.042 ± 0.070	0.484%	0.469%	0.454%	0.651%	0.678%	0.684%
		1.451	1.407	1.361	1.954	2.033	2.053

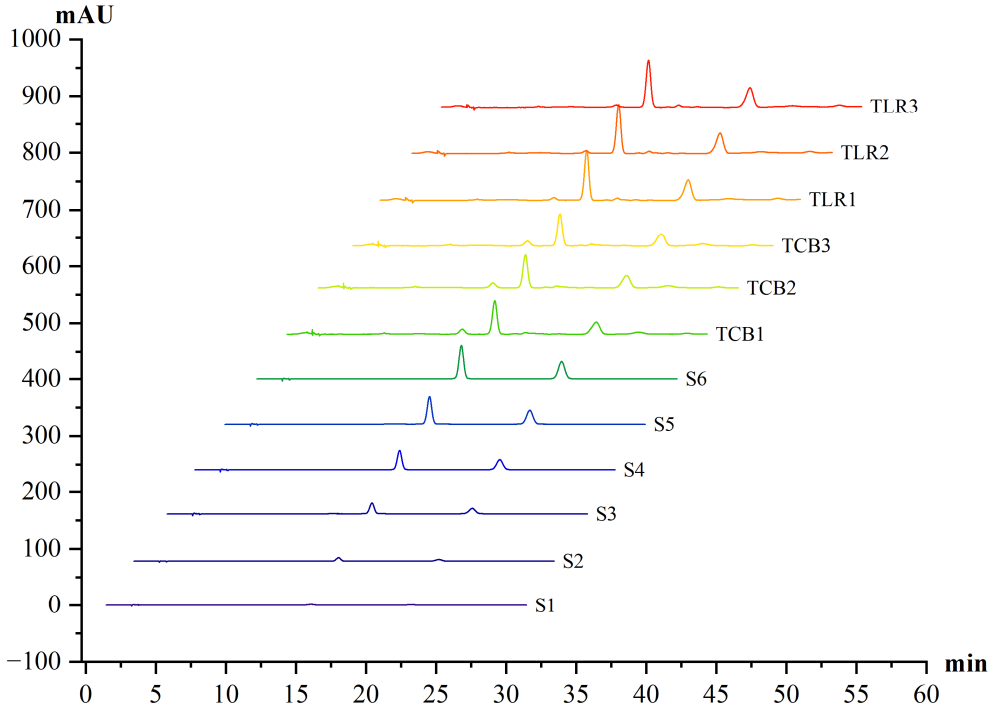


Figure 10. HPLC chromatograms of standards and sample extracts.

The HPLC chromatograms (Figure 10) showed several other peaks besides orientin and vitexin, indicating the presence of additional flavonoids or phenolic compounds in both TCB and TLR extracts. However, the current study focused on the quantification of

these two key marker compounds. The results indicate marginally higher concentrations of these components in TLR compared to TCB, suggesting that TLR may possess enhanced medicinal value and could serve as a viable alternative source of Flos Trollii.

4. Discussion

Flos Trollii primarily relies upon its active ingredients and pharmacological mechanisms of action, which provide substantial evidence supporting its practical applications. However, the high medicinal value of Flos Trollii has resulted in significant degradation of its original source, TCB, causing resource depletion and a continuous increase in market prices. Thus, there is an urgent need to identify alternative sources of medicinal herbs. TLR, a unique local medicinal herb native to the Great Xing'an Mountains in Heilongjiang Province, exhibits high quality but low yield due to geographic and environmental factors. Despite its potential, research on TLR remains limited, hindering the development of the TLR herb industry. This study aims to utilize physicochemical and botanical methodologies to analyze the similarities between TLR and TCB. Liquid chromatography analysis, performed in accordance with Pharmacopoeia standards and literature review, was conducted to determine the orientin and vitexin content. This approach is expected to facilitate the sustainable exploitation of high-quality Flos Trollii.

Morphologically, the most significant differences between the two species are observed in their floral structures, particularly in the length and number of calyx and petals. According to the study, the calyx of TLR is shorter than the petals. In contrast, the petals and calyx of TCB are nearly equal in length, with the petals slightly longer than the calyx and marginally shorter than the sepals. In full bloom, the flowers of TLR and TCB display notable similarities, in their morphology, characterized by yellow sepals that maintain their coloration upon desiccation; however, the sepals of TCB are marginally darker. Both species feature elliptic or obovate outer sepals with rounded apices, although TLR lacks the inconspicuous dentition present in TCB. The calyx lengths in both species exhibit variability, with TCB measuring between 1.2 and 2.5 cm, while TLR ranges from 1.2 to 3 cm. TCB is distinguished by having 18 to 21 petals marked with stripes and stamens ranging from 5 to 11 mm in length. In contrast, TLR possesses 10 to 22 petals exceeding the length of its stamens, which measure approximately 9 mm. The number of carpels in both species ranges from 20 to 30. Differences in fruit morphology between the two species are minimal, primarily relating to length.

In this study, the characterization and identification of botanical materials began with a rapid preliminary differentiation of TCB and TLR herbal powders based on macroscopic coloration. Subsequent microscopic examination provided anatomical reference data for both species. Although TCB and TLR exhibit considerable similarities in microscopic characteristics, consistent with their close taxonomic relationship, key diagnostic features were identified. These features include calyx epidermal cells with anomocytic stomata, spiral vessels, and unicellular trichomes, consistent with previous studies. Such characteristics help establish a standard authentication profile for genuine Flos Trollii.

Furthermore, microscopic evaluation provides a reliable method for detecting adulteration. Commercial samples lacking these diagnostic structures or containing unidentified elements may be considered adulterated or of inferior quality. Although microscopic analysis alone cannot fully differentiate between TCB and TLR, it remains essential as part of a comprehensive identification strategy. This approach ensures accurate and dependable quality assessments of medicinal materials. Classical taxonomic methods based on microscopic and macroscopic features have recently become less effective due to insufficient taxonomic expertise. This challenge is particularly evident when distinguishing between inclusions of TCB and TLR during microscopic identification. The phenomenon arises

because individuals of the same species can exhibit variable morphological traits influenced by environmental and other factors, complicating identification [26]. Additionally, closely related species or populations with minor differences, such as those within the genus *Trollius*, pose challenges when identified solely by morphology. This difficulty arises because morphological traits among these populations often exhibit minimal or negligible differences [27]. Fresh plants can be accurately identified through morphological features; however, dried flowers are often damaged and thus challenging to identify accurately. Consequently, additional identification methods are necessary to improve accuracy [28].

The development of molecular plant identification utilizing DNA barcodes has emerged as a robust method for identifying and characterizing mixed artifacts in herbal samples [29]. Specific regions of chloroplast and nuclear genomes, including *psbA-trnH*, *ycf1*, *ITS*2, and *trnL-trnF*, have been recommended as supplementary DNA barcodes for plant identification. ITS2 and *psbA-trnH*, in particular, have been extensively studied and validated as complementary markers. Additionally, *trnL-trnF* serves as an auxiliary resource to further validate the results [6,30,31]. In plant taxonomy, no single DNA region provides adequate species differentiation. Multiple experimental studies have demonstrated that a multi-labeling approach can enhance the result resolution and reliability [32,33]. Given the low intraspecific variability observed in plants, employing multiple DNA barcode markers increases the likelihood of accurate identification at the species level. For instance, researcher [34] utilized nuclear DNA sequences (*ITS*1, 5.8S, and *ITS*2) along with chloroplast DNA sequences (*trnL* introns and *trnL-trnF*) and Amplified Fragment Length Polymorphism (AFLP), to elucidate phylogenetic relationships within the genus *Trollius*. They combined chloroplast DNA markers (matK and trnL-F), nuclear DNA markers (ITS), and 17 morphological traits to investigate the phylogenetic relationships of *Trollius*. Similarly, researcher screened 12 highly variable plastid DNA barcode regions for species identification within the genus Aurelia, including *ndhC-trnV*, *rpl32-trnL*, *rps16-trnQ*, *trnE-trnT*, *ycf4-cemA*, *ycf1-ndhF*, *ycf1*, *trnK-rps16*, *ndhF-rpl32*, *psbM-trnD*, *ccsA*, *hD*, and *matK*. In the present study, a multi-marker approach utilizing *ITS*2, *psbA-trnH*, and *trnL-trnF* was employed to identify TCB and TLR.

Barcode gap analysis clearly demonstrates that the *psbA-trnH* intergenic spacer is the most effective DNA barcode for distinguishing within the genus Trollius, exhibiting a distinct gap with no overlap between intra- and inter-specific distributions. This conclusion is strongly supported by the genetic distance calculations between the two key species, TCB and TLR. The interspecific divergence between TCB and TLR in the *psbA-trnH* region (0.1576) was substantially greater than those in the ITS2 (0.0014) and *trnL-trnF* (0.0026) regions. This significant divergence, an order of magnitude higher than that observed in other barcodes, provides a decisive molecular basis for distinguishing these two morphologically similar species.

Notably, the observed asymmetry in psbA-trnH distances (TLR vs. TCB = 0.1576 vs. TCB vs. TLR = 0.0244) likely reflects underlying evolutionary rate heterogeneity between the two lineages, a frequent occurrence in chloroplast DNA evolution. Despite this intralocus variation, both values significantly exceed the maximum intra-specific variation recorded for either species, ensuring reliable identification.

In contrast, the ITS2 and trnL-trnF markers, while ubeneficial for broader phylogenetic analyses, proved insufficient for distinguishing TCB and TLR. The interspecific distances for both regions were extremely low and fell well within the range of intra-specific variation observed across the entire genus. This lack of divergence, coupled with extensive overlap in their respective violin plots, confirms that neither region possesses sufficient resolution for species-level discrimination between TCB and TLR.

Flavonoids are a class of low molecular weight polyphenolic compounds characterized by a 15-carbon flavan skeleton, which consists of two phenyl rings connected by a propane bridge (C_6-C_3-C_6) [35]. They are ubiquitously distributed throughout the plant kingdom. A diverse array of chemical constituents has been isolated from Flos Trollii, with numerous studies indicating that flavonoids represent the most abundant and biologically active components. A total of 28 flavonoid parent structures and approximately 98 flavonoid monomers have been identified [36]. Among flavonoids, orientin and vitexin are prominent compounds exhibiting diverse biological properties. Both belong to the flavone C-glycoside family and are widely distributed across multiple plant families [37]. As major structural derivatives of glycosylated flavonoids C-glycosylflavones have attracted significant interest due to their broad spectrum of biological activities, including antiviral, antibacterial, and antioxidant properties, demonstrating significant inhibitory effects against *Pseudomonas aeruginosa*, *Dysentery bacillus*, and *Staphylococcus aureus*, particularly in the context of upper respiratory tract infections caused by these susceptible bacteria, such as acute suppurative tonsillitis, pharyngitis, and otitis media. Additionally, they show promising therapeutic effects on acute enteritis and urinary infections [38]. Notably, orientin and vitexin are not only the major bioactive components in Flos Trollii but also coexist in plants such as bamboo leaves. Orientin has been identified in a wide range of medicinal plants, including but not limited to *Polygonum orientale* L. (Polygonaceae), *Mauritia flexuosa* L. (Arecaceae), *Passiflora coerulea* L. (Passifloraceae), *Scorzonera austriaca* Wild. (Asteraceae), *Phyllostachys heterocycla* (Poaceae), *Aspalathus linearis* (Fabaceae), *Ocimum sanctum* L. (Lamiaceae), *Leonurus cardiaca* L. (Lamiaceae), *Oxalis* L. (Oxalidaceae), and *Cecropia pachystachya* (Urticaceae), among others [39]. The content of orientin varies considerably among species. For example, in *Polygonum orientale*, it ranges from 0.0536% to 0.9260%, while in TCB, it varies between 0.19% and 3.69%. In *Phyllostachys heterocycla*, orientin constitutes approximately 0.03316%, and in *Indocalamus longiauritus*, about 0.0527%. Although qualitative analyses have confirmed the presence of orientin in other species such as *Jatropha gossypiifolia* and *Commelina communis*, quantitative data are not yet fully reported. It is noteworthy that in some plants, including certain Oxalis species, orientin represents the predominant flavonoid [40].

Similarly, vitexin is found not only in Flos Trollii but also in pearl millet, hawthorn, pigeon pea, mung bean, mosses, Passiflora, bamboo, mimosa, wheat leaves, and chaste tree or chasteberry in seeds, fruits, flowers, leaves, roots, etc. Mainly plant source of vitexin so far is hawthorn leaves. Vitexin concentration varies substantially among plant species, ranging from 0.00053% to 9.53%. The highest levels are found in Crataegus pinnatifida, particularly in its leaves [41]. Although qualitative analyses have confirmed the presence of orientin in other species such as *Jatropha gossypiifolia* and *Commelina communis*, quantitative data are not yet fully reported. It is noteworthy that in some plants, including certain Oxalis species, orientin represents the predominant flavonoid [39]. Owing to their valuable medicinal properties, orientin and vitexin are increasingly used in the pharmaceutical industry, making them a current research focus in the field of natural product chemistry [42]. The developed TLC method exhibits excellent resolution and reproducibility, confirming its suitability for the rapid identification and semi-quantitative analysis of orientin and vitexin in Trollius-based samples. TFC between TCB and TLR and HPLC results indicated that the content of Orientin and Vitexin in TLR was slightly higher than that in TCB. These findings suggest that TLR shows comparable flavonoid content and deserves further investigation as a potential alternative, and in certain instances, may possess superior medicinal or therapeutic efficacy. This study has several limitations that should be acknowledged. The conclusions are drawn from a limited sample size from specific regions, potentially overlooking intraspecific variation. The chemical analysis was also narrowed to flavonoids (orientin and vitexin), leaving a broader metabolomic profile unexplored. Consequently,

the pharmacological equivalence between TLR and TCB remains unvalidated without bioactivity assays. In this study, HPLC quantification revealed that TLR contained slightly higher levels of orientin (5.370–5.377 mg/g) and vitexin (1.954–2.053 mg/g) compared to TCB (orientin: 4.493–4.620 mg/g; vitexin: 1.361–1.451 mg/g). Although systematic quantitative data on these compounds across different plant species are currently lacking, it is known that C-glycosylflavones generally occur at levels below 1% (often 0.01–0.1%) in most medicinal plants. This indicates that both Trollius species, especially TLR, are enriched sources of orientin and vitexin. Further cross-species quantitative studies are needed to better define their phytochemical profiles. The elevated levels of orientin and vitexin in TLR are noteworthy, as these compounds are well-documented to possess significant antioxidant and anti-inflammatory activities [43]. This phytochemical profile suggests that TLR may possess comparable or enhanced bioactivity, a premise that aligns with findings in other medicinal plants where specific flavonoid enrichment correlates with higher antioxidant potential [44]. Therefore, future studies are warranted to expand on these findings through population-wide sampling strategy to assess intraspecific variation, untargeted metabolomics (e.g., UPLC-MS/MS), and essential bioactivity tests to rigorously compare the efficacy of TCB and TLR extracts. Therefore, future studies are warranted to expand on these findings through a multi-faceted approach: (1) a population-wide sampling strategy to comprehensively assess intraspecific chemical and genetic variation; (2) untargeted metabolomic profiling (e.g., using UPLC-MS/MS) to fully characterize the phytochemical composition beyond flavonoids; and (3) essential bioactivity tests, such as in vitro antioxidant (e.g., DPPH, ABTS, FRAP assays), anti-inflammatory (e.g., inhibition of NO production in LPS-induced macrophages), and antimicrobial assays against common respiratory pathogens. These direct comparisons of the efficacy of TCB and TLR extracts are critical to further validate their pharmacological equivalence and therapeutic potential.

5. Conclusions

This research undertook a comparative analysis of the similarities between TCB and TLR across four dimensions: morphological characteristics, microscopy, DNA barcoding, and the assessment of physicochemical component content. A thorough evaluation of these two species was conducted. The comparisons based on morphological characteristics, microscopy, and chloroplast DNA barcode regions (*psbA-trnH* and *trnL-trnF*) successfully discriminated between TCB and TLR, revealing notable differences between the two species within the genus *Trollius*, while the nuclear ITS2 marker showed limited resolution, consistent with the high genetic similarity within this genus HPLC analysis demonstrated that the concentrations of the primary active components in both species surpassed the standards established by the pharmacopoeia. The levels of active components were found to be comparable between the two species, with TLR exhibiting marginally higher concentrations than TCB. This suggests that TLR may possess enhanced biological activity. These findings provide a scientific basis for the medicinal utilization of TLR.

Author Contributions: L.H. and P.W.: designed and carried out the experiments, analyzed the data, and wrote the manuscript. Z.W. and L.K.: designed the study, wrote and revised the manuscript; J.M., S.H., M.P. and K.Y. wrote and revised the manuscript; W.L. and W.M.: designed the study; reviewed and edited the paper; X.L.: designed the study; wrote and revised the manuscript. All authors have read and agreed to the published version of the manuscript.

Funding: This work was supported by the Graduate Innovative Research Project of Heilongjiang University of Chinese Medicine, Science and Technology Plan of Heilongjiang Provincial Health Commission, and the National Key Research and Development Project, Research and Demonstration of Collection, Screening and Breeding Technology of Ginseng and other Genuine Medicinal Materials, Project (Grant numbers: 2024yjscx021, 20241313050309, and 2021YFD1600901).

Data Availability Statement: Data will be made available on request.

Conflicts of Interest: The authors declare that they have no known competing financial interests or personal relationships that could have appeared to influence the work reported in this paper.

Abbreviations

TCB	*Trollius chinensis* Bunge
TLR	*Trollius ledebouri* Rchb.
TAL	*Trollius asiaticus* L.
TFS	*Trollius farreri* Stapf
TMF	*Trollius macropetalus* (Regel) F.
*ITS*2	Internal Transcribed Spacer
LOD	Limit of detection
LOQ	Limit of quantification
RSD	Relative standard deviation
TFC	Total flavonoid content
$AlCl_3$	Aluminum chloride
NCBI	National Center for Biotechnology Information
PCR	Polymerase chain reaction
HPLC	High-Performance Liquid Chromatography
K2P	Kimura 2-parameter
ddH2O	Double-distilled water
NJ	Neighbor-Joining
AFLP	Amplified Fragment Length Polymorphism
TLC	thin-layer chromatography

References

1. Guo, M.L.; Xu, H.T.; Yang, J.J.; Chou, G.X. Diterpenoid glycosides from the flower of *Trollius chinensis* Bunge and their nitric oxide inhibitory activities. *Bioorg. Chem.* **2021**, *116*, 105312. [CrossRef]
2. He, L.; Wang, Z.; Lu, J.; Qin, C.; He, J.; Ren, W.; Liu, X. *Trollius chinensis* Bunge: A Comprehensive Review of Research on Botany, Materia Medica, Ethnopharmacological Use, Phytochemistry, Pharmacology, and Quality Control. *Molecules* **2024**, *29*, 421. [CrossRef]
3. Liang, J.W.; Wang, M.Y.; Olounfeh, K.M.; Zhao, N.; Wang, S.; Meng, F.H. Network pharmacology-based identifcation of potential targets of the flower of *Trollius chinensis* Bunge acting on anti-inflammatory effectss. *Sci. Rep.* **2019**, *9*, 8109. [CrossRef]
4. Li, J.; Du, Y.; Xie, L.; Jin, X.; Zhang, Z.; Yang, M. Comparative plastome genomics and phylogenetic relationships of the genus Trollius. *Front. Plant Sci.* **2023**, *14*, 1293091. [CrossRef]
5. Editorial Committee of the Flora of Reipublicae Popularis Sinicae, Chinese Academy of Sciences (Ed.) *Flora of Reipublicae Popularis Sinicae*; Science Press: Beijing, China, 1979; Volume 27, p. 86.
6. Lv, Y.N.; Yang, C.Y.; Shi, L.C.; Zhang, Z.L.; Xu, A.S.; Zhang, L.X.; Li, X.L.; Li, H.T. Identification of medicinal plants within the Apocynaceae family using ITS2 and psbA-trnH barcodes. *Chin. J. Nat. Med.* **2020**, *18*, 594–605. [CrossRef]
7. Bortiri, E.; Oh, S.-H.; Jiang, J.; Baggett, S.; Granger, A.; Weeks, C.; Buckingham, M.; Potter, D.; Parfitt, D.E. Phylogeny and Systematics of Prunus (Rosaceae) as Determined by Sequence Analysis of ITS and the Chloroplast trnL-trnF Spacer DNA. *Syst. Bot.* **2001**, *26*, 797–807.
8. Yan, R.; Cui, Y.; Deng, B.; Bi, J.; Zhang, G. Flavonoid glucosides from the flowers of *Trollius chinensis* Bunge. *J. Nat. Med.* **2019**, *73*, 297–302. [CrossRef]
9. Yang, K.; Wang, Z.; Wang, P.; Wang, L.; Li, Y.; He, L.; Liu, X.; Xu, J.; Duan, Y.; Ma, W. A Comprehensive Research Review of Herbal Textual Research, Phytochemistry, Pharmacology, Traditional Uses, Clinical Application, Safety Evaluation, and Quality Control of *Trollius chinensis* Bunge. *Pharmaceuticals* **2024**, *17*, 800. [CrossRef]
10. Wetters, S.; Horn, T.; Nick, P. Goji Who? Morphological and DNA Based Authentication of a "Superfood". *Front. Plant Sci.* **2018**, *9*, 1859. [CrossRef]
11. Su, Y.; Zhang, M.; Guo, Q.; Wei, M.; Shi, H.; Wang, T.; Han, Z.; Liu, H.; Liu, C.; Huang, J. Classification of *Isatis indigotica* Fortune and *Isatis tinctoria* Linnaeus via comparative analysis of chloroplast genomes. *BMC Genom.* **2023**, *24*, 465. [CrossRef]
12. Fan, Y.; Huang, L.; Su, S.; Su, S. Identification of Papaveraceae Based on Chloroplast DNA matK+rbcL+ trnH-psbA. *J. Kunming Med. Univ.* **2023**, *44*, 12–18. [CrossRef]

13. Gao, J.; Meng, W.-H.; Du, F.; Li, J. DNA Barcoding of *Acer palmatum* (Aceraceae). *J. Integr. Plant Biol.* **2015**, *33*, 734–743. [CrossRef]
14. Qin, X.; Jin, Y.; Gao, Z.; Wei, J. Identification of Cuscutae Semen and adulterants using DNA barcode. *Chin. Tradit. Herb. Drugs* **2024**, *55*, 5982–5990.
15. Xie, Q.; Zhang, H.; Yan, F.; Yan, C.; Wei, S.; Lai, J.; Wang, Y.; Zhang, B. Morphology and Molecular Identification of Twelve Commercial Varieties of Kiwifruit. *Molecules* **2019**, *24*, 888. [CrossRef] [PubMed]
16. Wen, R.; Yang, Y. Chromatographic Identification of the Active Components Orientin and Vitexin in *Flos trollii*. *Foreign Med. (Phytopharm. Issue)* **2008**, *23*, 2.
17. Yang, T.; Xiao, X.; An, Y.; Zhang, X. Research on Thin-Layer Identification and Content Determination of *Flos trollii*. *J. Pharm. Anal.* **2014**, *34*, 5.
18. Xie, Q. Study on Quality Standard and Phamacological Action from *Trollius ledebouri* Reichb. (Chinese Medicinal Herbs). Master's Thesis, Heilongjiang University of Chinese Medicine, Harbin, China, 2015.
19. Sun, P.; Li, X.; Xue, T.; Xin, J.; Liu, Y.; Chen, Y.; Guo, S.; Zhang, B. Research Progress on Identification and Quality Evaluation of *Trollius chinensis*. *Mod. Chin. Med.* **2022**, *24*, 2048–2054. [CrossRef]
20. Land, D.; Lu, M.; Yiziti, P.; Li, X.; He, W. Study on Microscopic Identification Characteristics and Optimal Extraction Process of Total Flavonoids from *Trollius chinensis* Bunge. *Xinjiang J. Tradit. Chin. Med.* **2016**, *34*, 61–64.
21. Zhang, D.; Alideltu, C.o. Research progress on *Trollius ledebouri* Rchb. *Chin. Tradit. Pat. Med.* **2016**, *38*, 2448–2453.
22. Wu, D. The Study of Plant Print Apparent Structural and System Evolution of 17 Genus in Ranunculaceae. Ph.D. Thesis, Northeast Normal University, Changchun, China, 2015.
23. Su, L.; Zhao, B. Microscopic identification of stems and leaves of *Trollius chinensis* Bunge. *China Tradit. Chin. Med. Sci. Technol.* **2016**, *23*, 176–177.
24. Lv, J.; Wang, X.; Feng, Y.; Li, Y.; Zhao, H.; Wang, Y. Effects of shading on the photosynthetic characteristics and anatomical structure of *Trollius chinensis* Bunge. *Acta Ecol. Sin.* **2012**, *32*, 6033–6043. [CrossRef]
25. Kaplan, Z. Phenotypic Plasticity in *Potamogeton* (*Potamogetonaceae*). *Folia Geobot.* **2002**, *37*, 141–170. [CrossRef]
26. Liu, Y. Morphological Variation and Population Genetic Research in Two Sympatric Quercus. Master's Thesis, Beijing Forestry University, Beijing, China, 2018.
27. Wang, L.; Huo, Z.; Xu, W.; Zhou, P.; Nan, W.; Guo, H.; Zhang, Q.; Yang, P.; Alolga, R.N.; Yin, X.; et al. Comparative plastomes of eight subgenus *Chamaesyce* plants and system authentication of Euphorbiae Humifusae Herba. *Food Chem.* **2024**, *447*, 139039. [CrossRef] [PubMed]
28. Mahima, K.; Sunil Kumar, K.N.; Rakhesh, K.V.; Rajeswaran, P.S.; Sharma, A.; Sathishkumar, R. Advancements and future prospective of DNA barcodes in the herbal drug industry. *Front. Pharmacol.* **2022**, *13*, 947512. [CrossRef]
29. Cabelin, V.L.; Alejandro, G.J. Efficiency of matK, rbcL, trnH-psbA, and trnL-F (cpDNA) to Molecularly Authenticate Philippine Ethnomedicinal Apocynaceae Through DNA Barcoding. *Pharmacogn. Mag.* **2016**, *12*, S384–S388. [CrossRef]
30. Chen, S.; Yao, H.; Han, J.; Liu, C.; Song, J.; Shi, L.; Zhu, Y.; Ma, X.; Gao, T.; Pang, X.; et al. Validation of the ITS2 region as a novel DNA barcode for identifying medicinal plant species. *PLoS ONE* **2010**, *5*, e8613. [CrossRef]
31. CBOL Plant Working Group; Hollingsworth, P.M.; Forrest, L.L.; Spouge, J.L.; Hajibabaei, M.; Ratnasingham, S.; van der Bank, M.; Chase, M.W.; Cowan, R.S.; Erickson, D.L.; et al. A DNA barcode for land plants. *Proc. Natl. Acad. Sci. USA* **2009**, *106*, 12794–12797. [CrossRef]
32. Arulandhu, A.J.; Staats, M.; Hagelaar, R.; Voorhuijzen, M.M.; Prins, T.W.; Scholtens, I.; Costessi, A.; Duijsings, D.; Rechenmann, F.; Gaspar, F.B.; et al. Development and validation of a multi-locus DNA metabarcoding method to identify endangered species in complex samples. *Gigascience* **2017**, *6*, gix080. [CrossRef]
33. Pamarthi, R.K.; Nagaraju, S.; Prasad, K.; Malav, P.K.; Nayar, E.R.; Panda, R.R.; Bhatt, K.C. Plant Taxonomy and Its Role in Studies of Plant Genetic Resources. In *Textbook of Plant Genetic Resources*; Tripathi, K., Gupta, V., Krishnappa, G., Kumari, J., Singh, G.P., Eds.; Springer: Singapore, 2025; pp. 7–43.
34. Cai, Y.-F.; Li, S.-W.; Chen, M.; Jiang, M.-F.; Liu, Y.; Xie, Y.-F.; Sun, Q.; Jiang, H.-Z.; Yin, N.-W.; Wang, L.; et al. Molecular phylogeny of Ranunculaceae based on rbc L sequences. *Biologia* **2010**, *65*, 997–1003. [CrossRef]
35. Zawawi, N.; Chong, P.J.; Mohd Tom, N.N.; Saiful Anuar, N.S.; Mohammad, S.M.; Ismail, N.; Jusoh, A.Z. Establishing Relationship between Vitamins, Total Phenolic and Total Flavonoid Content and Antioxidant Activities in Various Honey Types. *Molecules* **2021**, *26*, 4399. [CrossRef]
36. Qiu, Y. Study on the Extraction Process and Antibacterial Activity Evaluation of *Trollius chinensis* Bunge. Master's Thesis, South China University of Technology, Guangzhou, China, 2022.
37. Qiu, D.; Gong, C.; Wang, S.; Zhang, M.; Yang, C.; Wang, X.; Xiong, J. Recent Advances in 2D Superconductors. *Adv. Mater.* **2021**, *33*, e2006124. [CrossRef]
38. Sun, Y.; Li, Q.; Zhang, Q. Determination of orientin, vitexin and total flavonoids in *Trollius chinensis* from different areas and optimization of extraction process. *Northwest Pharm. J.* **2019**, *34*, 596–601.

39. Yu, Y.; Pei, F.; Li, Z. Orientin and vitexin attenuate lipopolysaccharide-induced inflammatory responses in RAW264.7 cells: A molecular docking study, biochemical characterization, and mechanism analysis. *Food Sci. Hum. Wellness* **2022**, *11*, 1273–1281. [CrossRef]
40. Ishaq, A.R.; El-Nashar, H.A.S.; Al-Qaaneh, A.M.; Asfandyar; Bashir, A.; Younis, T. Orientin: A natural glycoside with versatile pharmacological activities. *Nat. Prod. Res.* **2025**, *39*, 7180–7202. [CrossRef]
41. He, M.; Min, J.-W.; Kong, W.-L.; He, X.-H.; Li, J.-X.; Peng, B.-W. A review on the pharmacological effects of vitexin and isovitexin. *Fitoterapia* **2016**, *115*, 74–85. [CrossRef] [PubMed]
42. Yan, W.; Cheng, J.; Xu, B. Dietary Flavonoids Vitexin and Isovitexin: New Insights into Their Functional Roles in Human Health and Disease Prevention. *Int. J. Mol. Sci.* **2025**, *26*, 6997. [CrossRef] [PubMed]
43. An, F.; Yang, G.; Tian, J.; Wang, S. Antioxidant effects of the orientin and vitexin in *Trollius chinensis* Bunge in D-galactose-aged mice. *Neural Regen. Res.* **2012**, *7*, 2565–2575. [CrossRef] [PubMed]
44. Fahmy, M.I.; Sadek, M.A.; Abdou, K.; El-Dessouki, A.M.; El-Shiekh, R.A.; Khalaf, S.S. Orientin: A comprehensive review of a promising bioactive flavonoid. *Inflammopharmacology* **2025**, *33*, 1713–1728. [CrossRef]

Disclaimer/Publisher's Note: The statements, opinions and data contained in all publications are solely those of the individual author(s) and contributor(s) and not of MDPI and/or the editor(s). MDPI and/or the editor(s) disclaim responsibility for any injury to people or property resulting from any ideas, methods, instructions or products referred to in the content.